Incorporation of polymorphic spacers to inhibit sintering of $SrO/SrCO_3$ for thermochemical energy storage

by
Justin T. Tran

A THESIS

submitted to

Oregon State University

University Honors College

in partial fulfillment of
the requirements for the
degree of

Honors Baccalaureate of Science in Chemical Engineering
(Honors Scholar)

Honors Baccalaureate of Science in Sustainability
(Honors Scholar)

Presented June 2, 2017
Commencement June 2017

AN ABSTRACT OF THE THESIS OF

Justin T. Tran for the degree of Honors Baccalaureate of Science in Chemical Engineering and Honors Baccalaureate of Science in Sustainability presented on June 2, 2017.

Title: Incorporation of polymorphic spacers to inhibit sintering of $SrO/SrCO_3$ for thermochemical energy storage

Abstract approved:

_____

Nicholas J. AuYeung

Global energy needs are continuously increasing while fossil fuels remain an uncertain resource. With a growing population and demand for energy, alternative energy sources are being pursued to power the future. Fossil fuels are an unsustainable resource that brings along problems of climate change and atmospheric pollution. Concentrated solar power (CSP) is a promising method of converting solar energy into electricity while avoiding carbon emissions. Thermal energy storage (TES) in conjunction with CSP can increase efficiency in power generation and allow for generation beyond on-sun hours. One method of TES is thermochemical energy storage (TCES), which has potential for higher energy density. TCES is based storing energy chemical via reversible reactions. During peak sun hours, the endothermic reaction stores the thermal energy; thus, the reaction can be reversed to produce heat for off-peak sun hours.

One reaction that exhibits high energy densities is the reversible carbonation/ decomposition of $SrO/SrCO_3$, which occurs around 1200 °C. The reaction is nontoxic

and avoids the use of catalysts. The high reaction temperature leads to a higher Carnot efficiency for power generation, and could enable combined-cycle power production

Over many cycles, the material becomes less reactive due to sintering. Sintering inhibitors were looked at to determine if sintering could be hindered. Calcium sulfate and strontium phosphate were tested due to their inert nature and polymorphic properties.

Key Words: Concentrated Solar Power, Thermal Energy System, Sintering, Sustainability, Thermochemical

Corresponding e-mail address: tranju@oregonstate.edu

Incorporation of polymorphic spacers to inhibit sintering of $SrO/SrCO_3$ for thermochemical energy storage

by
Justin T. Tran

A THESIS

submitted to

Oregon State University

University Honors College

in partial fulfillment of
the requirements for the
degree of

Honors Baccalaureate of Science in Chemical Engineering
(Honors Scholar)

Honors Baccalaureate of Science in Sustainability
(Honors Scholar)

Presented June 2, 2017
Commencement June 2017

Honors Baccalaureate of Science in Chemical Engineering and Honors Baccalaureate of Science in Sustainability project of Justin T. Tran presented on June 2, 2017.

APPROVED:

Nicholas J. AuYeung, Mentor, representing Chemical Engineering

---

Chih-Hung Chang, Committee Member, representing Chemical Engineering

---

Fuqiong Lei, Committee Member, representing Chemical Engineering

---

Toni Doolen, Dean, University Honors College

I understand that my project will become part of the permanent collection of Oregon State University, University Honors College. My signature below authorized release of my project to any reader upon request.

Justin T. Tran, Author

Acknowledgements

I would like to thank the members of the AuYeung Research Group for assistance in setting up the TGA/DSC, ordering materials, and maintaining the equipment. In particular, I would like to thank Elham Bagherisereshki, Fuqiong Lei, Yige Wang, Griffin Drake, Daniel Vargas, Blake Lopez, and Jasper Limon. These individuals helped me become familiar with the lab space and molded me into the researcher I am today.

I would like to thank Dr. Nick AuYeung for all the support and guidance he has provided me throughout this process. He has always been encouraging me to pursue great opportunities ever since I reached out to him my sophomore year before he arrived in Corvallis. I thank him for making time in his busy schedule to help me and challenge me to critically think about my results.

I thank my parents for their unconditional support and love throughout my academic career. They have always supported me to pursue my dreams, whether that be in sports or academics. I can always count on them to be there for me when I need them.

Finally, I would like to acknowledge my partner Yuliya for being there with me ever since I first came to Oregon State University. She has always pushed me to work hard when adversity hit, such as results making no sense. She has believed in me ever since we first met as swimmers and has always wished for my success. I would not be here if it was not for her.

TABLE OF CONTENTS

Page

LIST OF FIGURES

Figure Page

LIST OF TABLES

Table Page

1. Background

There are two different ways of converting solar energy into electricity: photovoltaics and concentrated solar power (CSP). The former is most commonly seen in the form of solar panels, which converts solar energy directly to electricity. However, the latter first converts solar energy to thermal energy then to electricity. This leads to higher efficiency for power generation, but the technology is not commercially viable. Photovoltaics are the cheaper option but are less efficient than CSP systems.

Three types of solar collectors are commonly used to collect energy from the sun: solar trough, solar dish, and heliostat. For each, a concentration ratio *CR*, defined as the ratio of the aperture area to the receiver area, is used to maximize the amount of sunlight directed to the aperture from the receiver. The larger the *CR* the higher the efficiency will be. A trough typically has a *CR* that ranges from 10 – 50. A parabolic dish has a *CR* of 200 – 500. A heliostat has a *CR* of 500 – 3000, making heliostats the most efficient CSP technology. As *CR* increase, so does the operating temperature at the aperture. A trough operates at around 300 °C, a dish around 700 °C, and a heliostat around 900 °C.

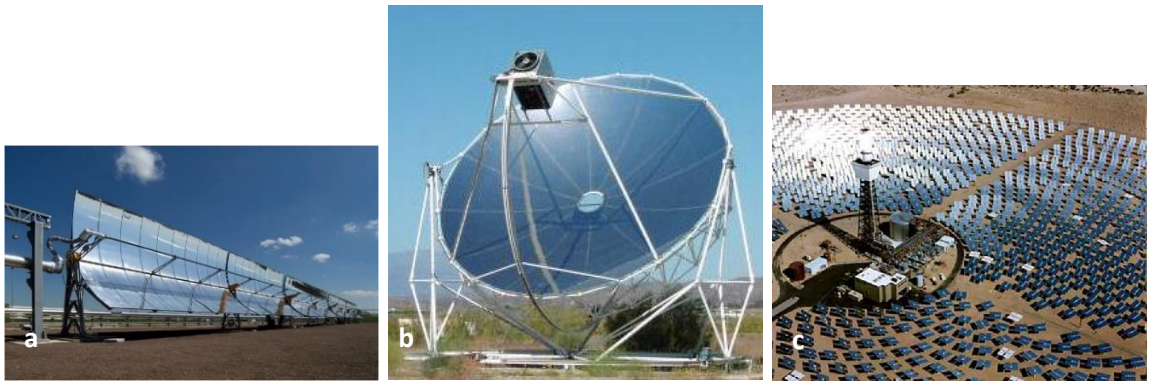

Figure 1: a. Parabolic solar trough.[1] b. Parabolic solar dish.[2] c. Heliostat array in California.[3]

CSP in conjunction with thermal energy storage (TES) can meet energy demands during the night when the sun no longer shines. There are three ways to store thermal energy: sensible heat storage, latent heat storage, and thermochemical energy storage (TCES). Sensible heat storage stores energy within a material by increasing its temperature. Latent heat stores energy within a phase change, such as evaporating liquid water into steam. TCES is when a reactive system absorbs thermal energy and proceeds with a reversible chemical reaction. The reaction can be reversed during off-sun hours to release energy. Of the three, TCES has the highest inherent energy density (Figure 2) and has the potential to translate into more competitive solar electricity prices.

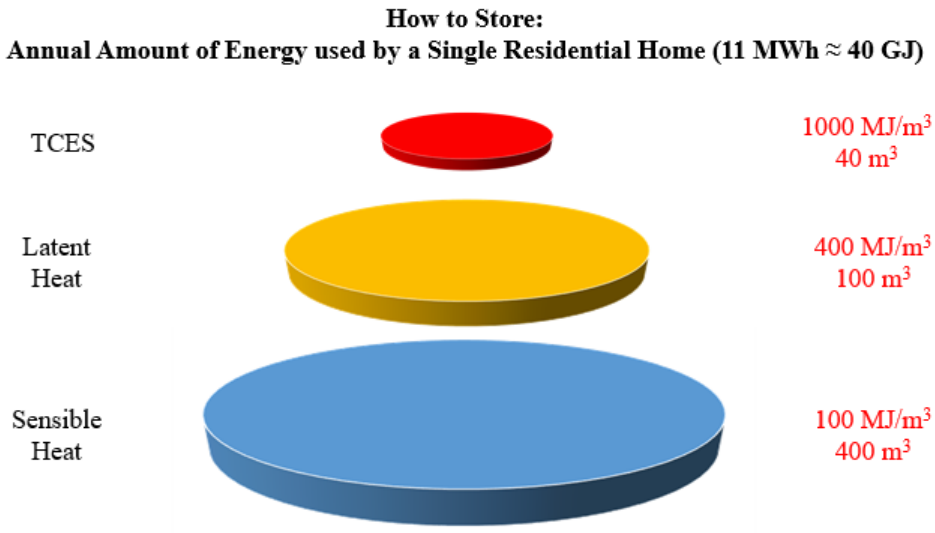

Figure 2: Volume needed to energize a home for a year using the three different thermal energy storages. TCES has the highest energy density, followed by latent heat, and the least is sensible heat.

1.1 Sensible Heat

Sensible heat is energy stored in a material that does not undergo a phase change as its temperature changes.[4] The amount of energy can be determined using the specific heat capacity of the material (Equation 1).

$$Q = \int_{T_i}^{T_f} mC_p(T)dT \quad (1)$$

Where Q is the amount of heat stored, m is the mass, C_p is the specific heat capacity as a function of T, and T is the temperature.

Potential materials for sensible heat storage are those with high specific heat capacities. Generally, sensible heat storage materials are classified into two groups: liquid or solid storage mediums. Liquid systems usually involve water or oil and solid systems involve rocks, bricks, concrete, molten salts, etc. Table 1 shows some commonly used solid and liquid materials used for sensible heat storage.

Table 1. Physical Properties of Various Liquid and Solids.[5,6,7,8]

Material	Type	Temperature Range (°C)	C_p [kJ/m-K]	k [W/m-K]
Water	Liquid	0 – 100	4.2	0.58
Ethanol	Liquid	Up to 78	2.4	0.17
Brick	Solid	20 – 70	0.84	1.2
Concrete	Solid	20 – 70	1.1	0.9 – 1.3
Granite	Solid	20 – 70	0.90	2.9

Commercially, molten salts have been used in conjunction with CSP, such as the Noor Concentrated Solar Power plant in Morocco. Molten salts typically used are sodium and potassium nitrates and they can store energy up to 550 °C. Concentrated solar is used to heat the molten salts as they move through the receiver and to an insulated storage tank. The collected heat can be stored until off-peak hours and then used to produce electricity in conjunction with the Brayton or Rankine cycle.[9]

1.2 Latent Heat

Latent heat storage is when heat is added to a material and it undergoes a phase change. The phase change may be solid-solid (change in crystal structure), solid-liquid,

solid-gas, liquid-gas, and vice-versa.[10] Higher latent heat values are found in solid-gas and liquid-gas transitions.[11]

Phase change materials used for latent heat storage can be classified as organic, inorganic, or eutectics.[12] Organic materials used are alkanes, fatty acids, alcohols, and esters. Inorganic materials include salt hydrates and metals.[10] Eutectics are a mixture of inorganic and organic compounds.

1.3 Thermochemical Energy Storage

High temperature TCES systems can be classified by their reaction family as metallic hydrides, carbonates, hydroxides, redox system, ammonia system, and organic system.[12] The most developed system is ammonia dissociation, which has been pilot tested. Moreover, the dehydration and hydration reaction of calcium hydroxide and calcium oxide has been studied as a potential system, but still has many barriers to overcome before it is pilot tested.[13]

Hygroscopic salts have shown good potential for storing heat through a dehydration reaction. Salts like calcium chloride, magnesium chloride, and magnesium sulfate have energy densities of 720, 2171, and 1512 MJ/m^3, respectively. These reactions occur at lower temperatures, generally around 100 – 150 °C.[12] Since the dehydration reactions occur at lower temperatures, it is more difficult to recover the heat discharged.

Calcium oxide has become an emerging reaction for thermochemical energy storage due to its cheap price and availability. Calcium oxide carbonates in the presences

of carbon dioxide to form calcium carbonate, an exothermic reaction, and then it calcinates back to calcium oxide, an endothermic reaction.

$$CaO(s) + CO_2(g) \leftrightarrow CaCO_3(s) \quad \Delta H^0_{298\,K} = -179\frac{kJ}{mol}$$

This process is commonly called calcium looping. Carbonation occurs at around 650 °C and calcination occurs at around 900 °C. Another motivation to use $CaO/CaCO_3$ is because calcium oxide acts as a carbon dioxide sorbent.[14] As fossil fuels continue to be used, more and more carbon dioxide will be emitted into the atmosphere, causing a need to find new uses with the excess carbon dioxide in the atmosphere.

A reversible reaction that is similar to calcium looping is strontium oxide carbonation and strontium carbonate decomposition:

$$SrO(s) + CO_2(g) \leftrightarrow SrCO_3(s) \quad \Delta H^0_{298\,K} = -234\frac{kJ}{mol}$$

This reaction occurs at higher temperatures as the exothermic carbonation occurs around 1150 °C and endothermic decomposition occurs around 1200 °C. The released heat from the carbonation reaction can be used for power generation., as shown in Figure 3. Higher temperatures lead to a higher efficiency for power generation, as shown in the Carnot Cycle and Carnot efficiency.

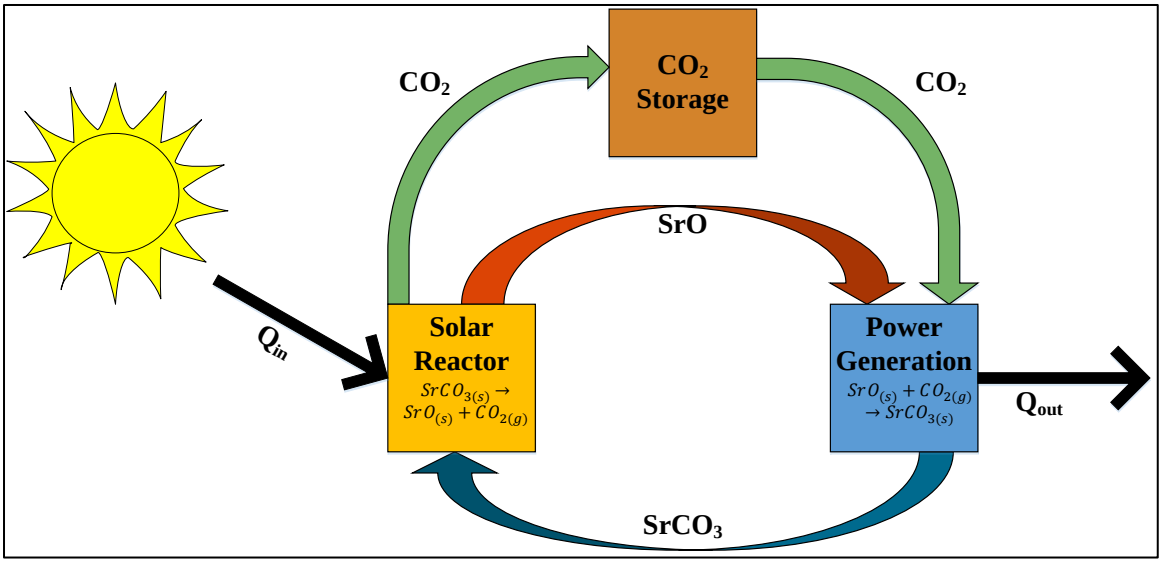

Figure 3: Schematic representation of SrO/$SrCO_3$ for power generation.

There are significant advantages of using SrO/$SrCO_3$ as compared to other TCES chemistries. First, it is a nontoxic and cheap material. Second, the reaction does not involve any catalyst and there are no side reactions or products.[15]

At high temperatures, sintering of strontium oxide occurs. Sintering is the physical aggregation of crystals that lead to increased particle size.[16] This reduces the surface area of the sorbent particles, leading to a decrease in reactivity. In order to prevent sintering, the sorbent may be doped with an inert material to prevent the crystals from aggregating.

Sintering of strontium oxide was found to be inhibited using an yttria-stabilized strontium zirconate support. The energy density with the zirconate support was 1500, 1430, and 1260 MJ/m^3 after 10, 15, and 45 cycles, respectively. However, zirconate is expensive, leading to the need of other supports.[16]

Polymorphic spacers have been used to inhibit sintering for calcium looping. Calcium silicate (Ca_2SiO_4) was used as a dopant since it undergoes a crystal structure

change between 660 – 930 °C, between carbonation and calcination of $CaO/CaCO_3$. The idea is that as the dopant changes crystal structures, it pushes the particles of $CaO/CaCO_3$ to maintain their size. The material is shown to be stable for 15 cycles when doped with a polymorphic spacer.[17]

Polymorphic spacers have not been studied with the carbonation and decomposition of $SrO/SrCO_3$. Since $SrO/SrCO_3$ occurs at higher temperatures, other polymorphs are needed to potentially synthesize sintering resistant sorbents. Two potential polymorphs that can be used with strontium oxide are calcium sulfate $CaSO_4$ and strontium phosphate $Sr_3(PO_4)_2$. Calcium sulfate was found to make a monazite- to barite-type transition at around 1230 °C.[18] This transition occurs right before decomposition occurs for $SrCO_3$, making it a potential sintering inhibitor. Furthermore, phosphates were investigated due to their known polymorphic behavior. Calcium phosphate undergoes a β- to α-type transition between 1140 – 1200 °C, after the carbonation temperature of 1150 °C.[19] Also, strontium phosphate is believed to undergo a similar transition as calcium phosphate since both materials are similar.[20]

With phase transitions between the carbonation and decomposition temperature of $SrO/SrCO_3$, calcium sulfate and strontium phosphate are hypothesized to inhibit sintering by maintaining particle size at high temperatures, as shown in Figure 4.

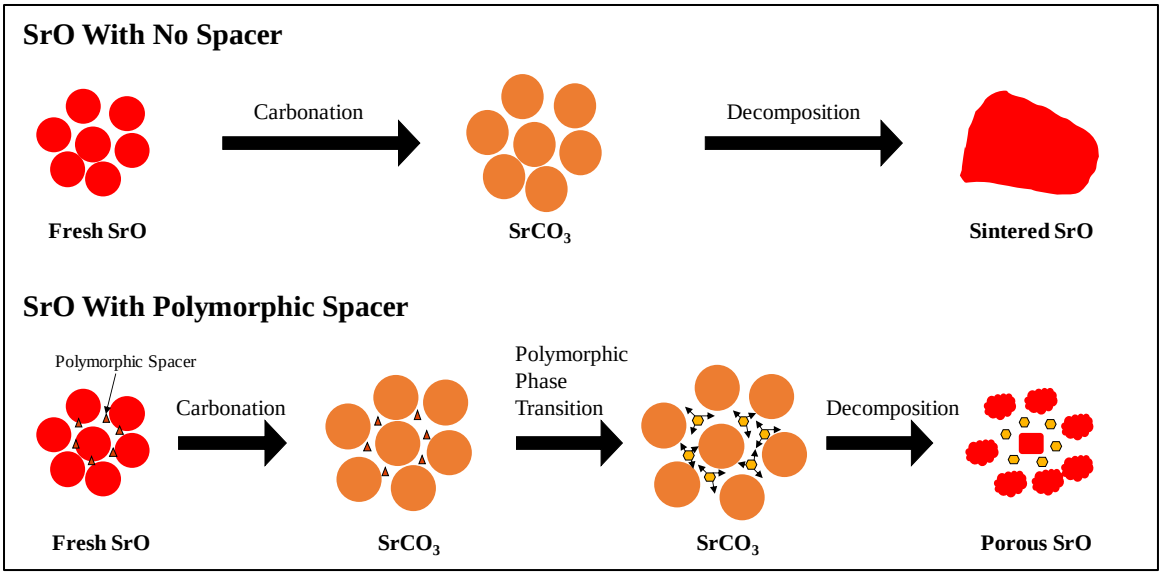

Figure 4: SrO is carbonated to SrCO3 and then decomposed to SrO. Without a dopant, SrO sinters after repetitive use. To reduce sintering, a polymorphic spacer is added to separate particles and push them back between cycles.

2. Experimental Section

2.1 Material Preparation

Strontium oxide (Alfa Aesar) was either undoped or mixed at various weight percent with calcium sulfate (J.T. Baker) or strontium phosphate (Sigma Aldrich) for testing. The mixture was heated in a muffle furnace (SentroTech ST-1600) at temperatures from 1400 - 1525 °C for 8 hours under air to ensure formation of large grains. The sample was then crushed with a mortar and pestle to create particles of various sizes. After crushing, the sample was sieved to particles size ranging from less than 25 μm, 25 - 53 μm, 53 - 75 μm, 75 - 106 μm, and greater than 106 μm.

Testing was done with particles sizes between 53 and 75 μm as it was found that initial particle size has little effect on the reaction kinetics.[21] Leftover sample was stored in an airtight container and stored in an airtight plastic bag to prevent it from absorbing moisture.

Strontium oxide is highly hygroscopic and quickly transforms into strontium hydroxide or a hydrate during the material synthesis. Therefore, the mass ratio of strontium oxide is unknown at the beginning of testing. An initial dehydration step at 1200 °C is done to dehydrate all strontium hydroxide to pure strontium oxide, as shown in Figure 5.

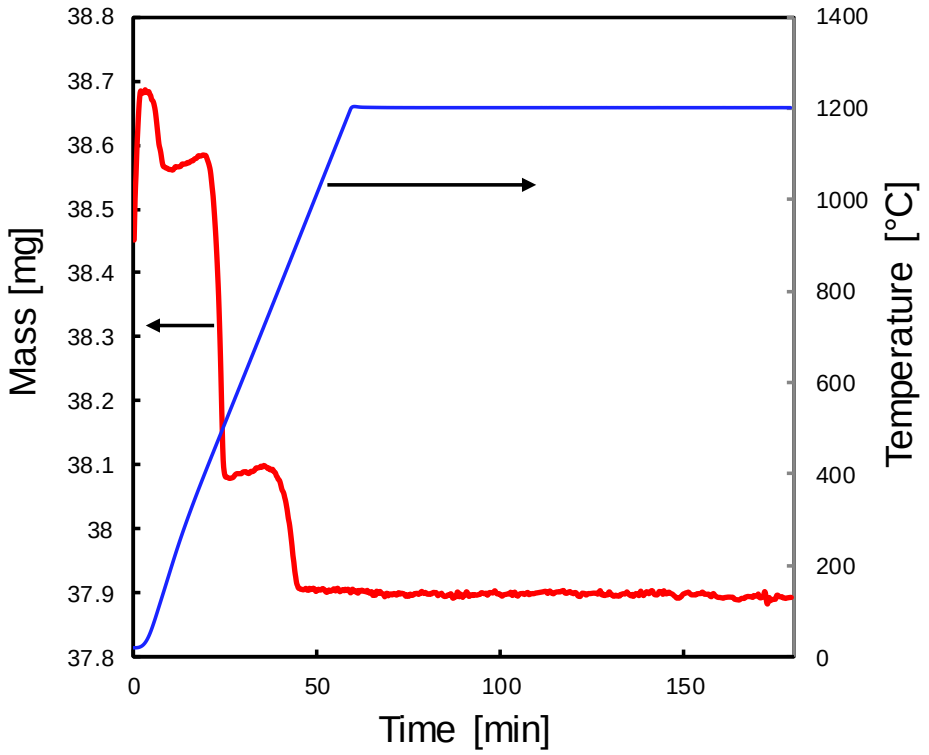

Figure 5: TGA data for one experiment to show the dehydration of strontium hydroxide during the initial dehydration step. The minimum mass achieved was assumed to be the mass of strontium oxide. Dehydration occurred under argon gas.

2.2 TGA Operation

Data was obtained by performing thermogravimetric analysis (TGA) and differential scanning calorimetry (DSC) using Netzsch STA449 F5 Jupiter.

A correction file was run prior to each experiment to correct for any phase changes that the alumina crucible may undergo. The correction file was done at the same conditions as experiments, with the only exception being that no sample was loaded. Each experiment was performed with approximately 40 mg of material loaded into an alumina crucible.

Since the mass of strontium oxide is unknown due to its hygroscopic nature, the sample was heated at 1200 °C for two hours under an inert atmosphere (argon) with a

flow rate of 40 mL/min. The temperature was then decreased to the carbonation temperature of 1150 °C. Carbon dioxide began flowing at 10 - 25 mL/min began upon reaching 1150 °C while inert flow was reduced to 5 - 20 mL/min. The total flow of carbon dioxide and argon remained constant at 30 mL/min during carbonation. The system remained at 1150 °C for 90 minutes to ensure carbonation of the strontium oxide.

The temperature was then increased to 1235 °C for decomposition of the newly formed strontium carbonate. The system remained isothermal for 30 minutes to ensure complete decomposition of strontium carbonate. Carbonation and decomposition were repeated for 10 - 30 cycles to see the effects of sintering over time. The temperature was increased and decreased at a rate of 20 K/min.

A series of experiments were carried out to determine the effects of pretreatment temperature, carbon dioxide flow rate, and various weight percent of strontium oxide doped with a polymorphic spacer. Energy densities were taken as kJ/kg rather than MJ/m^3 due to inconsistencies when determining the densities of samples. Densities were measured using the mass after the initial dehydration step and the volume, which was estimated using a caliper. Volumetric energy density was calculated using Equation 2 and gravimetric energy density was calculated using Equation 3.

$$Energy\ Density\ \left[\frac{MJ}{m^3}\right] = \frac{\Delta m \cdot \rho \cdot \Delta H^o_{rxn,25°C}}{M_{CO_2} \cdot m_i} \tag{2}$$

$$Energy\ Density\ \left[\frac{kJ}{kg}\right] = \frac{\Delta m \cdot \Delta H^o_{rxn,25°C}}{M_{CO_2} \cdot m_i} \tag{3}$$

Where Δm is the mass change, ρ is the density, $\Delta H^{o}_{rxn,25℃}$ is the standard heat of reaction, M_{CO_2} is the molecular weight of carbon dioxide, and m_i is the mass after the initial dehydration step.

3. Results and Discussion

3.1 Pre-heat treatment

Each sample is pretreated by placing it within a muffle furnace for eight hours to form large grains. Typically, samples are treated at 1500 °C due to preserve furnace lifetime. Since energy density is dependent on the sample's density post analysis, different temperatures of heat treatment were investigated. Three different treatment temperatures were looked at: 1400 °C, 1500 °C, and 1525 °C. All samples were strontium oxide with no spacer. Figure 6 shows the result of the three samples as well as an untreated sample over 10 cycles.

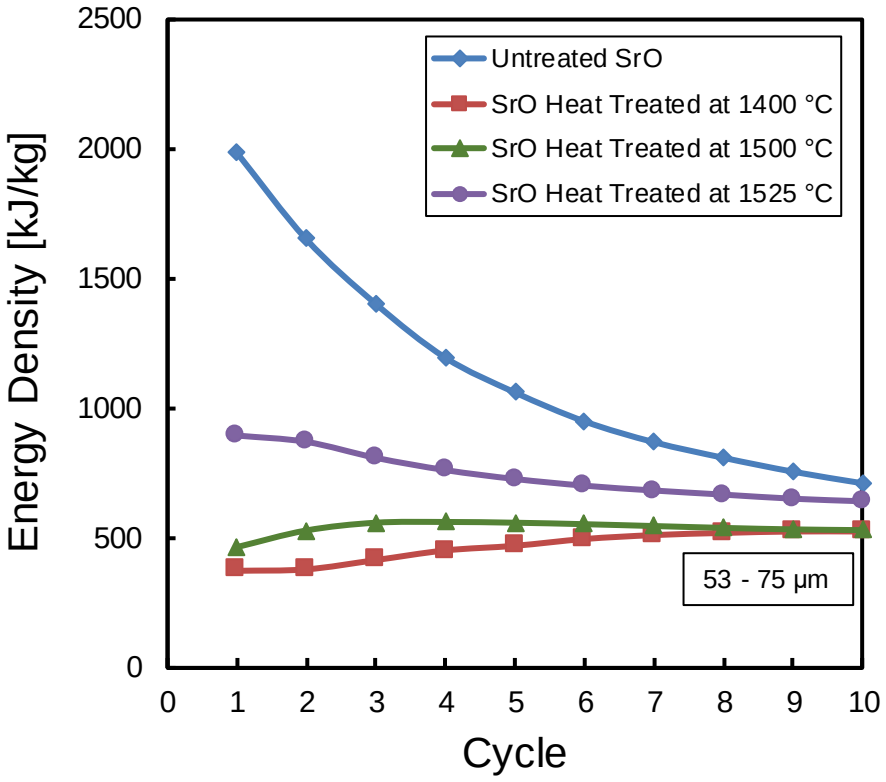

Figure 6: Energy density of samples of strontium oxide heat treated at different temperatures. Sintering is exhibited in the untreated sample while the treated sample showed some resistance to sintering.

At higher temperatures of heat treatment, the energy densities of the sample increase. After the first cycle, the energy density is lowest when the sample is treated at 1400 °C and highest for the untreated sample. After multiple cycles, sintering is experienced for the untreated sample and the sample treated at 1525 °C since the energy density decreases after each cycle. However, the two samples treated at 1400 and 1500 °C appear to be stable for 10 cycles.

The untreated sample initially has the highest energy density – up to 2000 kJ/kg. However, the energy density quickly decreased as more cycles are performed. This comes as a result of the untreated sample having fine particle sizes. Small particles cause the sample to sinter more rapidly, leading to the need of heat treatment.

Interestingly, the sample treated at 1400 °C shows an increase in energy density before it begins to stabilize at cycle seven, which could be due to limitations in mass transfer for carbon dioxide. Overall, treating samples at 1500 °C show the most promise, since the material appears to be stable over 10 cycles. However, it is hypothesized that the sample will experience sintering after 10 cycles due to the lack of a spacer.

3.2 Partial Pressure of Carbon Dioxide

The partial pressure of carbon dioxide was explored to see if oversaturating the system affects the energy density and sintering. An overall flow rate of 30 mL/min is ran during carbonation, but the ratio of carbon dioxide and argon were adjusted. Figure 7 explores the results from those tests.

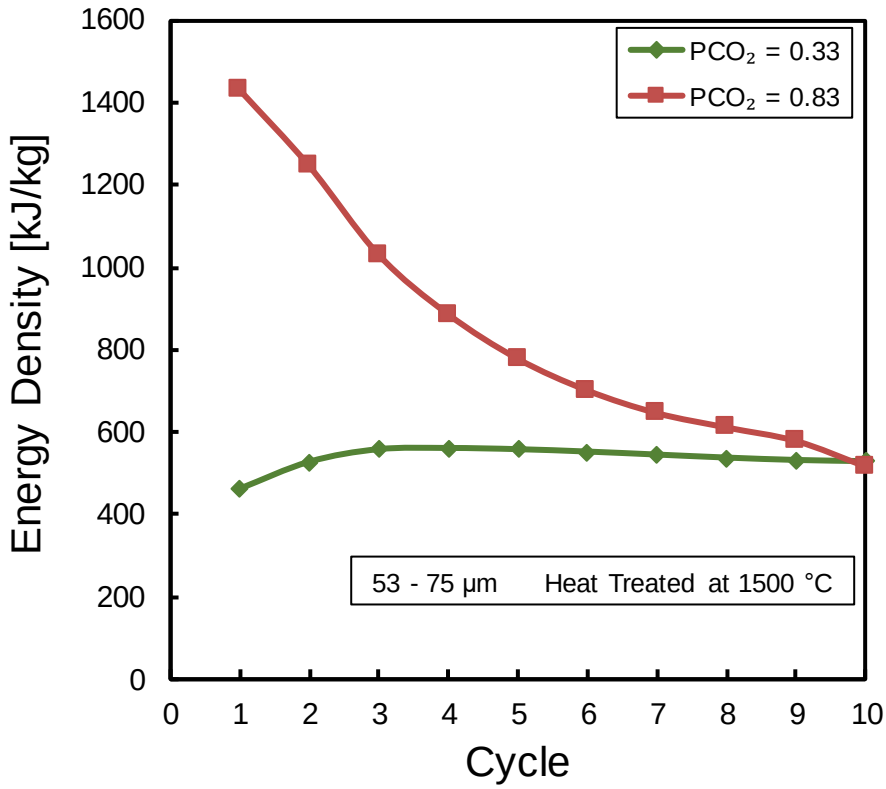

Figure 7: Energy density over 10 cycles for experiments with different CO_2 partial pressure. Each sample was heat treated at 1500 °C and was undoped.

At higher partial pressures, the energy density begins high but quickly decreases. At lower partial pressures, the energy density stabilizes after the third cycle. Although higher partial pressure causes a high initial energy density, lower partial pressures are favorable in inhibiting sintering since it appears to keep the sample stable through 10 cycles.

Since a lower partial pressure of carbon dioxide is favorable, less carbon dioxide would be needed in a closed system reactor. On a larger scale, carbon dioxide is stored after decomposition to a low temperature tank. Lower partial pressures mean the storage vessel would be less pressurized, resulting in cheaper costs.

3.3 Dopant Characterization

Calcium sulfate and strontium phosphate were both testing in the TGA to determine if and when they undergo a polymorphic transition. The sample was heated to 1300 °C at a rate of 20 K/min.

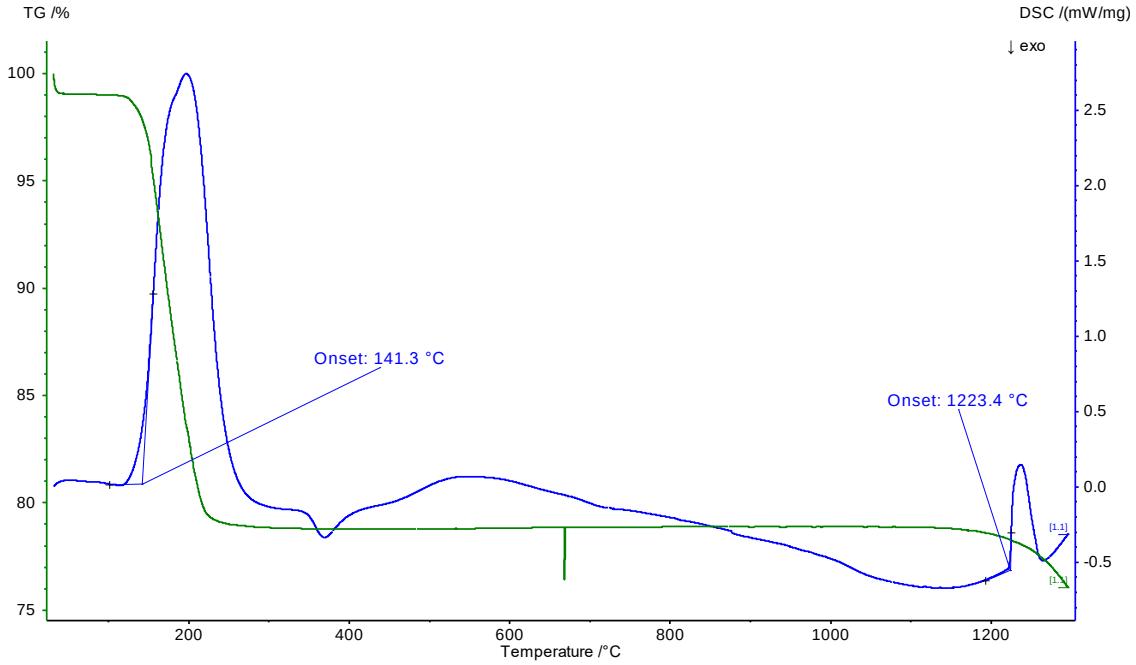

Figure 8. DSC and TGA curve for calcium sulfate when heating to 1300 °C.

The sample undergoes dehydration at around 141 °C and then remains relatively stable until 1220 °C, when it undergoes a transition. This transition is believed to be a polymorphic transition as calcium sulfate is reported to have much higher decomposition temperatures and the sample is tested until argon.[18] The TGA spike occurring around 700 °C is a result of the correction file.

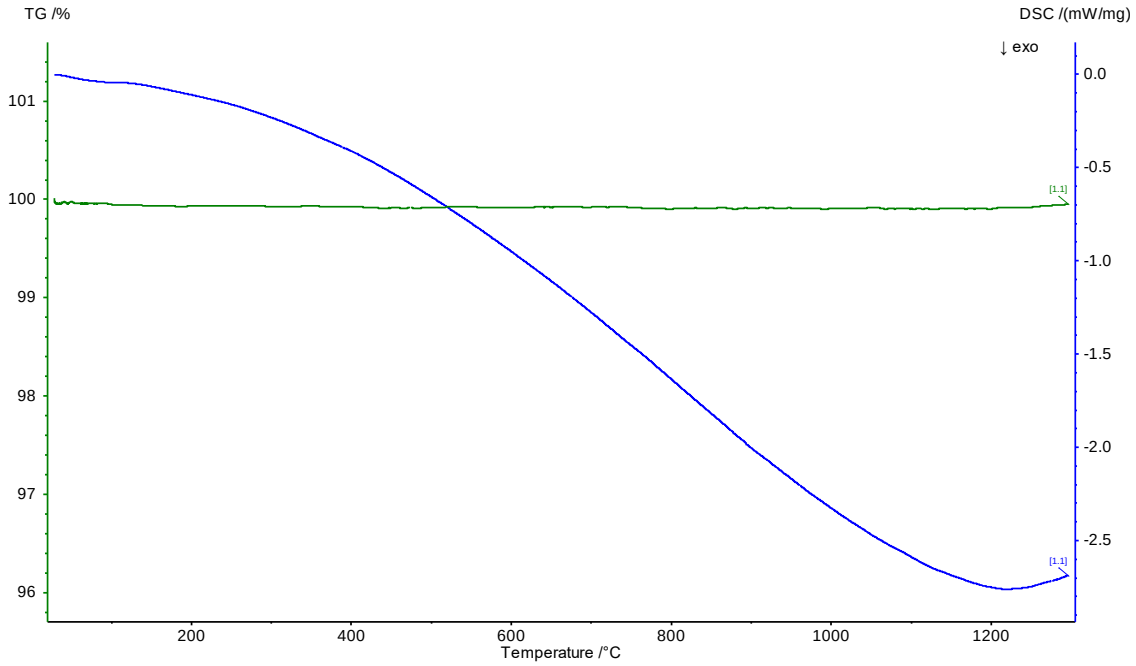

Figure 9. DSC and TGA curve for strontium phosphate when heating to 1300 °C.

The sample appears to undergo no transitions between 20 – 1300 °C. However, from the TGA curve, strontium phosphate remains stable at high temperatures and may work as a sintering inhibitor, but not as a polymorphic spacer. Both dopants will be further tested to see how they affect sintering of strontium oxide.

3.4 Strontium Oxide Doped with Polymorphic Spacer

Each dopant was initially tested at 50 wt% to determine if sintering could be hindered with a polymorphic spacer. Weight percent was chosen as a basis due to its simplicity in calculations and measurements. In Figure 10, the reaction appears to be stable through 10 cycles with polymorphs. This reveals that the strontium phosphate may work as a sintering inhibitor.

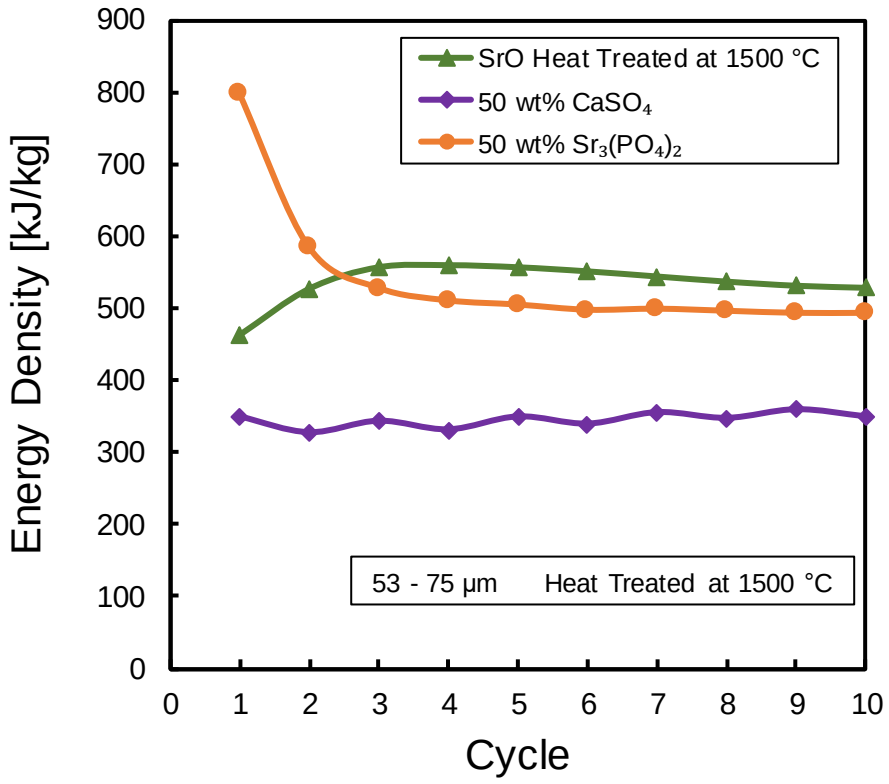

Figure 10: Energy density over 10 cycles for experiments for strontium oxide doped with a polymorphic spacer (calcium sulfate or strontium phosphate). Each sample was heat treated at 1500 °C. Undoped strontium oxide is used as a reference.

The calcium sulfate sample remains stable throughout the 10 cycles. However, the energy density is relatively low compared to strontium oxide with no dopant. This is a result of a lower percentage of reactive strontium oxide in the doped sample. Lower amounts of dopant will help increase the energy density; however, lower amounts of dopant could result in sintering.

The strontium phosphate sample also remains stable through 10 cycles. The energy density of the system with strontium phosphate is greater than the system with calcium sulfate by about 200 kJ/kg. Strontium oxide with strontium phosphate has a high initial energy density but it decreases after the first two cycles. Afterwards, the sample

stabilizes and is competitive with the undoped strontium oxide sample, as both have energy densities between 500 – 600 kJ/kg.

Although the undoped strontium oxide sample has comparable energy density to the doped sample and appears to be stable, it is speculated that longer testing will result in sintering due to the high temperatures and the lack of any type of dopant. Furthermore, since strontium oxide doped with strontium phosphate has a higher energy density than doping the material with calcium sulfate, strontium phosphate was further investigated at different ratios.

Strontium phosphate was further investigated at three different weight percents: 15, 25, and 50 wt%. At lower percentages of strontium phosphate, there is more reactive strontium oxide that will increase the energy density. The downside is that there is less spacer, increasing the chance for sintering. Figure 11 shows how different weight ratios of strontium phosphate to strontium oxide affect energy density.

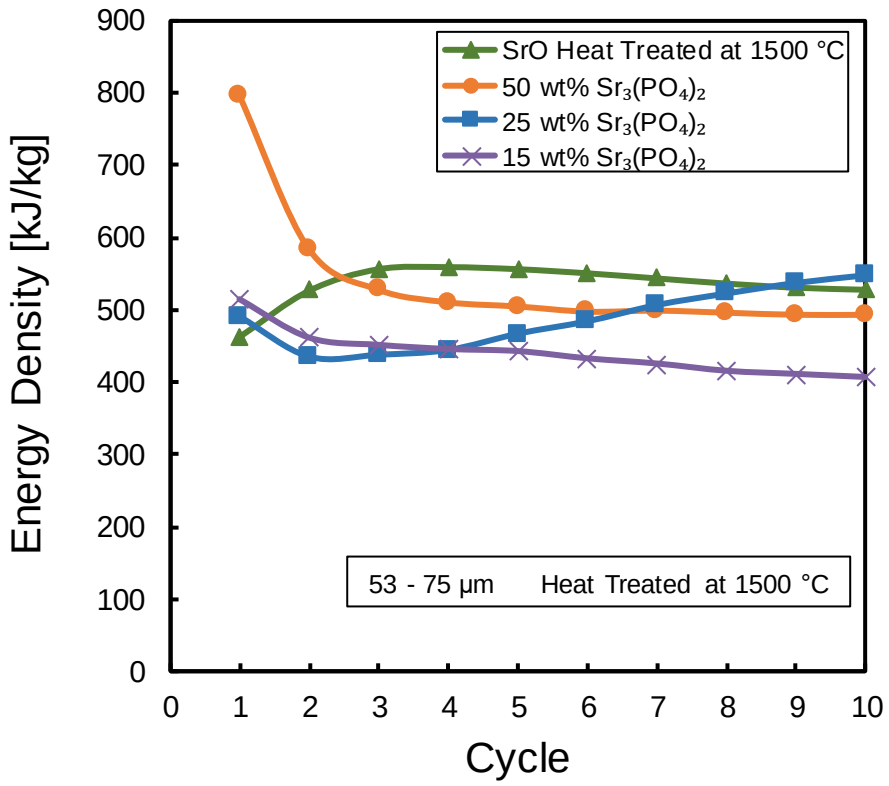

Figure 11: Energy density of samples with different ratios of strontium phosphate. Undoped strontium oxide at 1500 °C is used as a reference.

The energy density is higher at 25 wt% than it is for 50 wt% at the end of the 10 cycles. The lowest ratio of strontium phosphate of 15 wt% shows evidence of sintering, showing a similar trend as the undoped sample. The energy density of the sample with 25 wt% strontium phosphate shows a gradual decrease during the first two cycles and then is increases in the subsequent cycles. This causes it to overcome the energy density of 50 wt% at cycle seven. The increase in energy density may be due to mass transfer limitations of carbon dioxide, and further testing is needed to be done to see if the increase in energy density is consistent.

3.5 X-Ray Diffraction

Following heat treatment of each sample, they were tested using D8-Discover X-Ray Diffractometer to determine the XRD spectra. The identity of the sample was determined with the spectra and to ensure that no reaction occurred between the sample and dopant.

The spectra were run between 20 to 70 2θ and compared to the spectra for strontium oxide, calcium sulfate, and strontium phosphate. The spectra (Figure 12) reveal that strontium oxide, strontium hydroxide, and the dopant are present within the sample. All peaks for strontium oxide are present. Due to strontium oxide's hygroscopic nature, a lot of peaks that appear in the spectra are from strontium hydroxide or a hydrate.

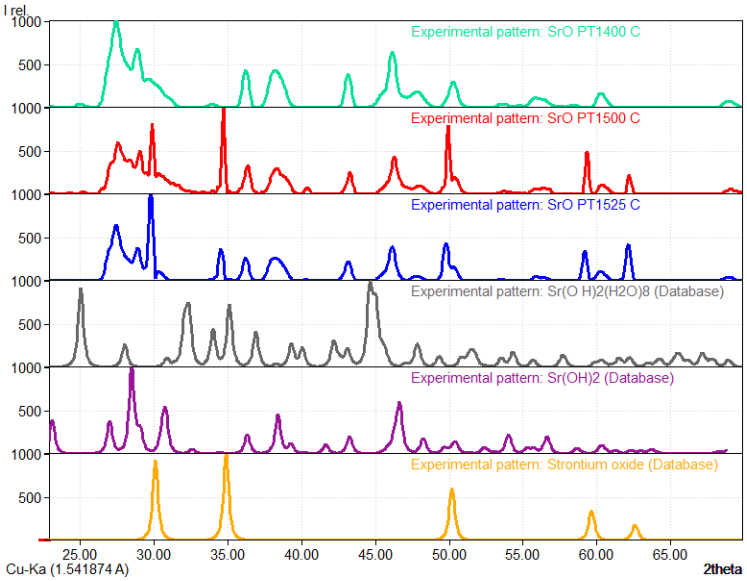

Figure 12: XRD spectra for strontium oxide heat treated at 1400, 1500, and 1525 °C from 20 – 70 2θ. All strontium oxide peaks are present. Peaks for strontium hydroxide and its hydrates are present as well.

3.6 Optimal Conditions

The optimum weight percent of strontium phosphate was found to be 25 wt%. This was tested for 30 cycles to see if the sample remains stable for longer periods. Figure 13 shows the results from the 30 cycle test.

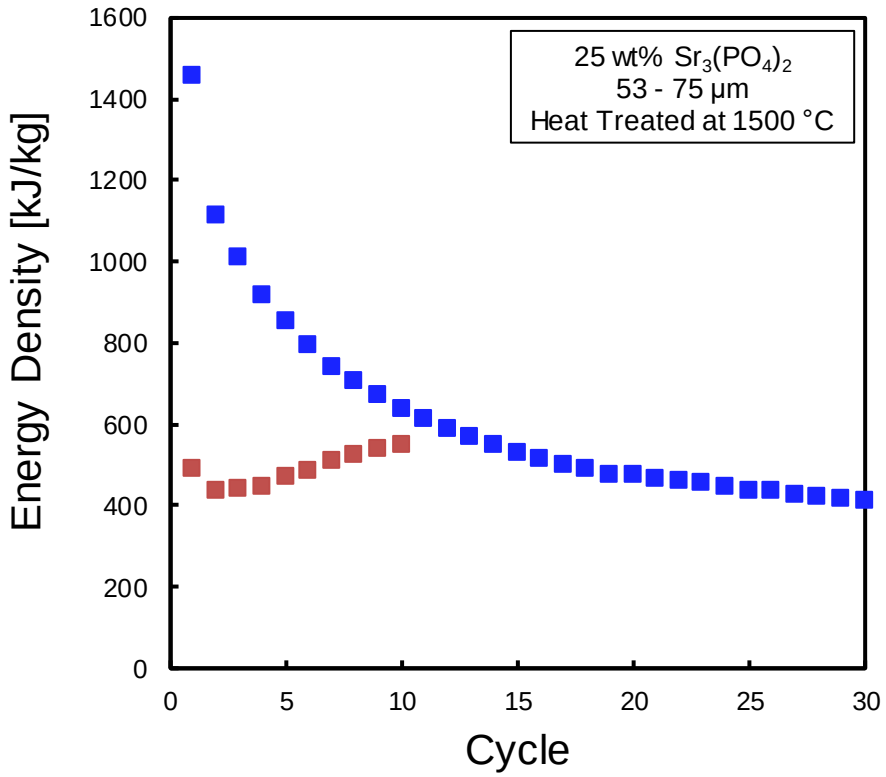

Figure 13: Strontium oxide with 25 wt% strontium phosphate over 10 and 30 cycles. Both samples were treated the same.

For the doped sample, the energy density starts at 1450 kJ/kg for the 30 cycle test, greater than the 10 cycle test by 1000 kJ/kg. The energy density is not consistent between the 30 cycles as the lowest energy density is 400 kJ/kg, much lower than the starting point. The trend for the 30 cycle test resemble the trend seen by the untreated undoped strontium oxide sample in Figure 6. The change in trend may be attributed to a change in

particle size in the sample as it becomes hydrated due to its hygroscopic nature, so further investigation was done.

3.7 Reproducibility

Following the 30 cycle test, it is believed that as the sample absorbs moisture from the atmosphere, the particles change in size. This was tested by running replicates of the 1500 °C heat treated sample. Two more tests were conducted from the sample that came from the same batch as the first test, but has been stored for one month. Another test was run from a fresh sample that was heat treated within 24 hours of testing. Results are found in Figure 14.

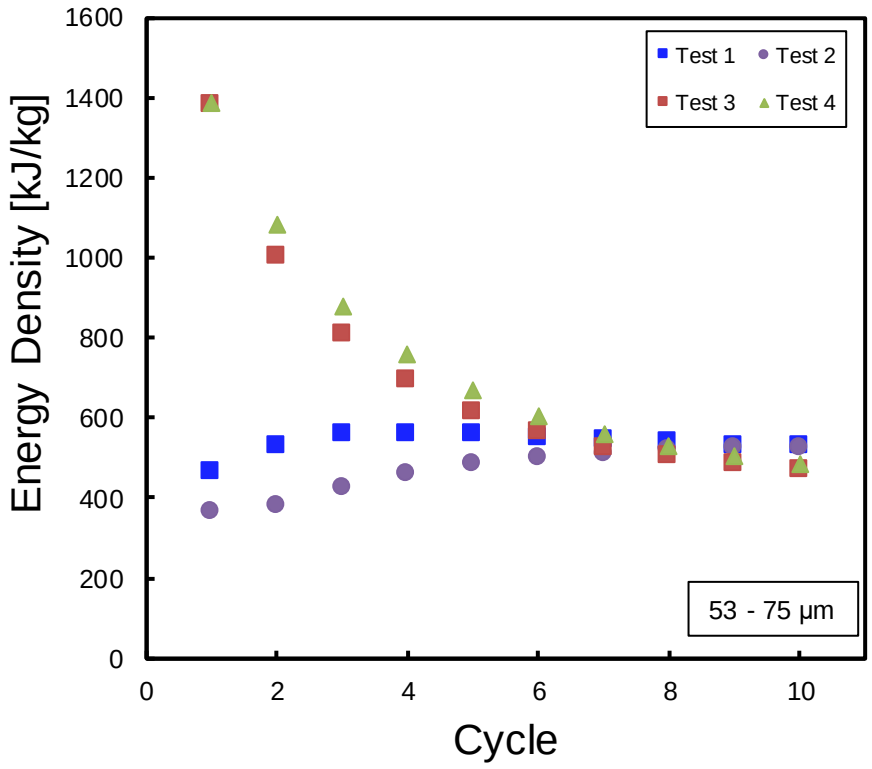

Figure 14: Energy density of strontium oxide heat treated at 1500 °C for four separate trials. Tests 1 and 2 were conducted within 24 hours of heat treatment and tests 3 and 4 were conducted one month after heat treatment.

Two trends are seen in Figure 14: one where energy density quickly decreases with cycles and one where energy density increases in the first two to three cycles and then stabilizes. The former is seen with samples that are tested a month after heat treatment and the latter is seen with samples that are tested within 24 hours of heat treatment. When a sample is stored for prolonged periods of time, it absorbs moisture from the air and becomes strontium hydroxide or a hydrate.

A sample was re-sieved after being stored for a month and it was found that the particle sizes changed. The sample was originally sieved and stored to be between 53 to 75 μm. When it was re-sieved, the particles ranged from 25 – 106 μm, as seen in Figure 15.

Figure 15: Distribution of particle sizes for a sample of strontium oxide that has been stored for one month after heat treatment and initially being sieved to 53 – 75 μm. Distribution of new particle sizes are from 25 – 53, 53 – 75, and 75 – 106 μm.

The amount of moisture absorbed by the strontium oxide can be determined from the initial dehydration step during tests (Figure 15). The percent hydration for the four tests were determined by the following equation:

$$\%\, Hydration = \frac{\Delta m}{m_i} \times 100\% \quad (4)$$

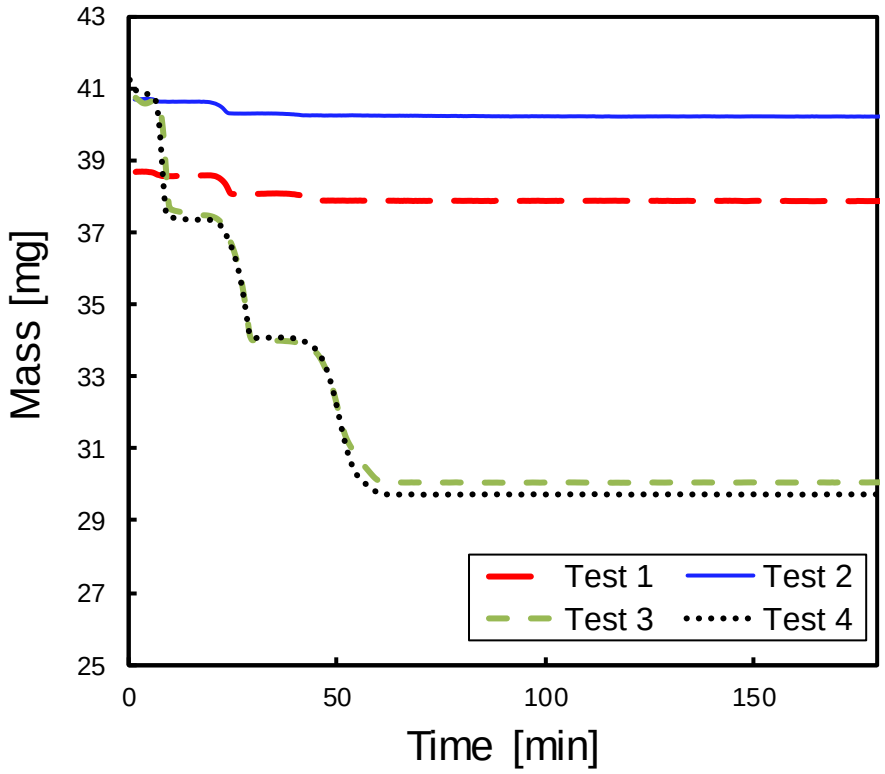

Figure 16: TGA Data for the four different tests during the initial dehydration step. Tests 1 and 2 show that the sample was not highly hydrated, whereas tests 3 and 4 were highly hydrated.

From Figure 16, it is seen that tests 3 and 4 were more hydrated than tests 1 and 2. The samples used for tests 1 and 2 were 2.2 and 1.2% hydrated, respectively. The samples used for tests 3 and 4 were 26 and 27% hydrated, respectively.

At high percent hydration (above 20%), the particle size of strontium oxide change, allowing it to initially be more reactive. This allows for sintering to take place after multiple cycles.

3.8 Hydration

Hydration was reevaluated for previous tests to confirm results. Summary of the results can be found in Table 2.

Table 2. Summary of all experiments done with percent hydration of the sample to validate results.

Sample	% Hydration	Figure Reference
Untreated SrO	42.5%	6
SrO Heat Treated at 1400 °C	0.6%	
SrO Heat Treated at 1500 °C Test 1	2.2%	
SrO Heat Treated at 1525 °C	7.5%	
$P_{CO_2} = 0.33$	2.2%	7
$P_{CO_2} = 0.83$	30.4%	
SrO Heat Treated at 1500 °C Test 1	2.2%	10
50 wt% $CaSO_4$	19.5%	
50 wt% $Sr_3(PO_4)_2$	11.1%	
SrO Heat Treated at 1500 °C Test 1	2.2%	11
50 wt% $Sr_3(PO_4)_2$	11.1%	
25 wt% $Sr_3(PO_4)_2$	1.6%	
15 wt% $Sr_3(PO_4)_2$	2.3%	
25 wt% $Sr_3(PO_4)_2$ 10 Cycles	1.6%	13
25 wt% $Sr_3(PO_4)_2$ 30 Cycles	22.7%	
SrO Heat Treated at 1500 °C Test 1	2.2%	14
SrO Heat Treated at 1500 °C Test 2	1.2%	
SrO Heat Treated at 1500 °C Test 3	26.0%	
SrO Heat Treated at 1500 °C Test 4	27.1%	

The only tests where there are huge discrepancies between percent hydration is the testing of the effects of carbon dioxide partial pressure and the 30 cycle test. The two samples from the partial pressure test differed in percent hydration by about 28 %. For

the 30 cycle test, the sample was 20 % more hydrated than the sample used for the 10 cycle test. These tests need to be repeated with samples that are low in moisture to ensure accuracy. All other results are validated.

4. Conclusions

Concentrated solar power (CSP) in conjunction with thermal energy storage (TES) can reduce the dependence on fossil fuels and increase the feasibility of solar energy by enabling operators to generate electricity beyond normal on-sun hours. One type of TES is thermochemical energy storage (TCES), which is based on a reversible reaction. This type of TES has the highest energy density as compared to the other two TES systems - sensible heat storage and latent heat storage.

X-ray diffraction and thermogravimetric analysis (TGA) were used to study the effects of doping strontium oxide with a polymorphic spacer (calcium sulfate) and sintering inhibitor (strontium phosphate). The goal of the spacer is to hinder sintering by being a physical barrier between the strontium oxide particles that would keep particles intact either as the barrier undergoes a phase change or acting as a barrier.

Pretreating strontium oxide at higher temperatures increased energy density up to 1500 °C. Temperatures above that cause samples to experience sintering. Calcium sulfate and strontium phosphate were both found to hinder sintering, but strontium phosphate resulted in a higher energy density when at the same weight percent. Further testing of strontium phosphate showed that an optimum amount of the dopant was 25 weight percent. The percent hydration of the sample prior to testing has an effect on particle size and sintering. When samples are less hydrated, they are more likely to be stable compared to highly hydrated samples. Strontium phosphate in conjunction with a low moisture content shows inhibition of sintering.

5. References

[1] Parabolic trough http://www.archimedesolarenergy.it/parabolic_trough_archimede.htm

[2] Solar Dish Collector used in a Solar Hot Water System http://www.alternative-energy-tutorials.com/solar-hot-water/solar-dish-collector.html

[3] NMT Heliostat Project http://infohost.nmt.edu/~helio/background.html

[4] Fernandez, A.; Martínez, M.; Segarra, M.; Martorell, I.; Cabeza, L. Selection of materials with potential in sensible thermal energy storage. *Solar Energy Materials and Solar Cells* **2010**, *94* (10), 1723–1729.

[5] Wilson, J. Thermal Diffusivity http://www.electronics-cooling.com/2007/08/thermal-diffusivity/

[6] Atear, O.E. Storage of thermal energy. Encyclopedia of life support systems (EOLSS). **2008**.

[7] Asan, H.; Sancaktar, Y.S. Effects of 'wall's thermophysical properties on time lag and decrement factor. *Energy and Buildings* **1998**, *28*, 159–166.

[8] Barreira, E.; deFreitas, V.P. Evaluation of building materials using infrared thermography. *Construction and Building Materials* **2007,** *21*, 218–224.

[9] Piemonte, V.; Falco, M. D.; Tarquini, P.; Giaconia, A. Life cycle assessment of a high temperature molten salt concentrated solar power plant. *Solar Energy* **2011**, *85* (5), 1101–1108.

[10] Sharma, A.; Tyagi, V.V.; Chen, C.R.; Buddhi, D. Review on thermal energy storage with phase change materials and applications. *Renewable and Sustainable Energy Reviews* **2009**, *13*, 318-345

[11] Hasnain, S. Review on sustainable thermal energy storage technologies, Part I: heat storage materials and techniques. *Energy Conversion and Management* **1998**, *39* (11), 1127–1138.

[12] Tatsidjodoung, P.; Pierrès, N. L.; Luo, L. A review of potential materials for thermal energy storage in building applications. *Renewable and Sustainable Energy Reviews* **2013**, *18*, 327–349.

[13] Pardo, P. *et al.* A review on high temperature thermochemical heat energy storage. *Renew. Sustain. Energy Rev.* **32,** 591–610 (2014).

[14] Kierzkowska, A. M.; Pacciani, R.; Muller, C. R. CaO-Based CO_2 Sorbents: From Fundamentals to the Development of New, Highly Effective Materials. *ChemSusChem* **2013**, *6*, 1130–1148.

[15] Arvanitidis, I.; Seetharaman, S.; Xiao, X. Effect of Heat and Mass Transfer on Thermal Decomposition of $SrCO_3$ Compacts. *Metallurgical and Materials Transactions B* **1999**, *30* (5), 901–908.

[16] Rhodes, N. R.; Barde, A.; Randhir, K.; Li, L.; Hahn, D. W.; Mei, R.; Klausner, J. F.; AuYeung, N. Solar Thermochemical Energy Storage Through Carbonation Cycles of $SrCO_3$/SrO Supported on $SrZrO_3$. *ChemSusChem* **2015**, *8*, 3793-3798.

[17] Zhao, M.; Shi, J.; Zhong, X.; Tian, S.; Blamey, J.; Jiang, J.; Fennell, P. S. A novel calcium looping absorbent incorporated with polymorphic spacers for hydrogen production and CO2 capture *Energy Environ. Sci.* **2014**, *7* (10), 3291–3295.

[18] Fujii, T.; Ohfuji, H.; Inoue, T. Phase relation of $CaSO_4$ at high pressure and temperature up to 90 GPa and 2300 K. *Physics and Chemistry of Minerals* **2016**, *43* (5), 353–361.

[19] Maciejewski, M.; Brunner, T. J.; Loher, S. F.; Stark, W. J.; Baiker, A. Phase transitions in amorphous calcium phosphates with different Ca/P ratios. *Thermochimica Acta* **2008**, *468* (1-2), 75–80.

[20] Zhai, S.; Xue, W.; Yamazaki, D.; Shan, S.; Ito, E.; Tomioka, N.; Shimojuku, A.; Funakoshi, K.-I. Compressibility of strontium orthophosphate $Sr_3(PO_4)_2$ at high pressure. *Physics and Chemistry of Minerals* **2010**, *38* (5), 357–361.

[21] Bagherisereshki, E. Carbonation Kinetics of SrO By CO_2 for Solar Thermochemical Energy Storage. Thesis.

6. Appendix

6.1 X-Ray Diffraction

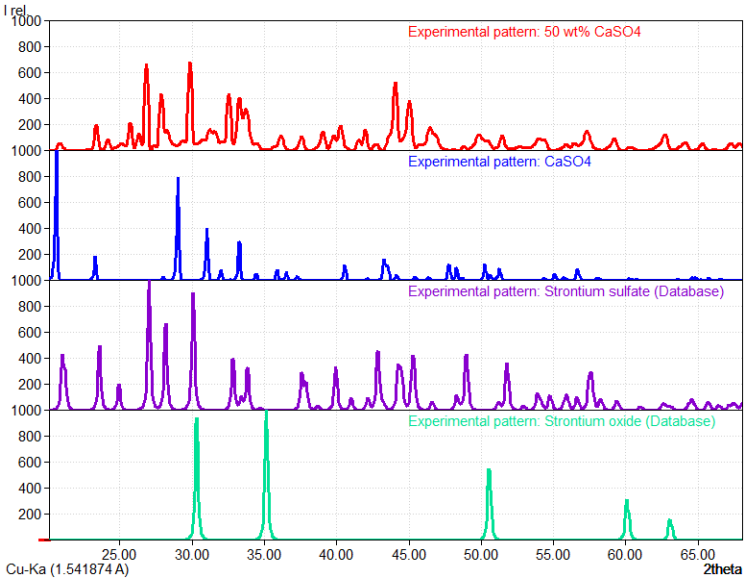

Figure 17: XRD Spectra for SrO doped with $CaSO_4$.

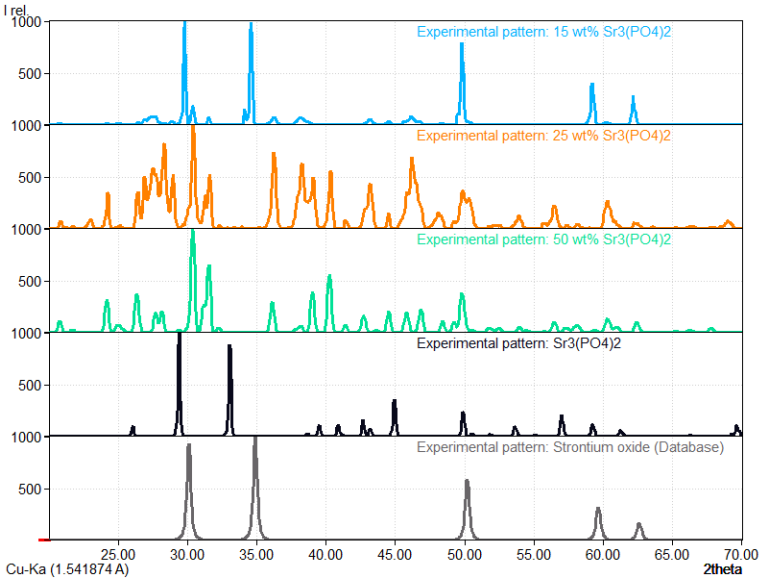

Figure 18: XRD Spectra for SrO doped with $Sr_3(PO_4)_2$.

6.2 Instrument Setup

Table 3: Program file used for experiments

Segment	Starting Temperature	Ramp Rate	Isotherm Time (hh:mm)	Ending Temperature
1	16°C	20.0 K/min		1200°C
2	1200°C		2:00	1200°C
3	1200°C	20.0 K/min		1150°C
4	1150°C		1:30	1150°C
5	1150°C	20.0 K/min		1235°C
6	1235°C		0:30	1235°C
7	1235°C	20.0 K/min		1150°C
8	1150°C		1:30	1150°C
9	1150°C	20.0 K/min		1235°C
10	1235°C		0:30	1235°C
11	1235°C	20.0 K/min		1150°C
12	1150°C		1:30	1150°C
13	1150°C	20.0 K/min		1235°C
14	1235°C		0:30	1235°C
15	1235°C	20.0 K/min		1150°C
16	1150°C		1:30	1150°C
17	1150°C	20.0 K/min		1235°C
18	1235°C		0:30	1235°C
19	1235°C	20.0 K/min		1150°C
20	1150°C		1:30	1150°C
21	1150°C	20.0 K/min		1235°C
22	1235°C		0:30	1235°C
23	1235°C	20.0 K/min		1150°C
24	1150°C		1:30	1150°C
25	1150°C	20.0 K/min		1235°C
26	1235°C		0:30	1235°C
27	1235°C	20.0 K/min		1150°C
28	1150°C		1:30	1150°C
29	1150°C	20.0 K/min		1235°C
30	1235°C		0:30	1235°C
31	1235°C	20.0 K/min		1150°C
32	1150°C		1:30	1150°C
33	1150°C	20.0 K/min		1235°C
34	1235°C		0:30	1235°C
35	1235°C	20.0 K/min		1150°C
36	1150°C		1:30	1150°C
37	1150°C	20.0 K/min		1235°C
38	1235°C		0:30	1235°C
39	1235°C	20.0 K/min		1150°C
40	1150°C		1:30	1150°C
41	1150°C	20.0 K/min		1235°C
42	1235°C		0:30	1235°C